Journal of Volcanology and Geothermal Research 303 (2015) 79–91

Contents lists available at ScienceDirect

Journal of Volcanology and Geothermal Research

journal homepage: www.elsevier.com/locate/jvolgeores

Submarine explosive volcanism in the southeastern Terceira Rift/São Miguel region (Azores)

B.J. Weiß [a,*], C. Hübscher [a], D. Wolf [a,b], T. Lüdmann [c]

[a] Institute of Geophysics, University of Hamburg, Bundesstrasse 55, D-20146 Hamburg, Germany
[b] Now at Polarcus Limited, Almas Tower, Level 32, Jumeirah Lakes Towers, PO Box 283373, Dubai, United Arab Emirates
[c] Institute of Geology, University of Hamburg, Bundesstrasse 55, D-20146 Hamburg, Germany

ARTICLE INFO

Article history:
Received 26 March 2015
Accepted 27 July 2015
Available online 4 August 2015

Keywords:
Azores
Bathymetry
Backscatter
Multi-channel seismic
Volcanic cones
Submarine explosive volcanism

ABSTRACT

Morphologic studies with sonar data and in situ observations of modern eruptions have revealed some information suggesting how submarine volcanic cones develop, but the information only addresses the modern surfaces of these features. Here, we describe a study combining morphological data with high-resolution seismic reflection data collected over cones within the southeastern Terceira Rift — a succession of deep basins, volcanic bathymetric highs and islands (e.g. São Miguel) representing the westernmost part of the Eurasian–Nubian plate boundary. The cones (252) are distributed in depths down to 3200 m and exhibit an average diameter of 743 m, an average slope of 20° and heights mainly between 50 and 200 m. The cones are here classified into three different categories by physiographic or tectonic setting (we find no particular morphometric differences in cone shapes between these areas). First, numerous cones located at the submarine flanks of São Miguel's Sete Cidades and Fogo Volcano are considered to be parasitic structures. Second, in the southeast of the island, they form a superstructure possibly reflecting an early submarine stadium of a posterior subaerial stratovolcano. Third, some cones are controlled by faults, mostly in a graben system southwest of the island. High-resolution multichannel seismic data indicates that the graben cones evolved synchronously with the graben formation. Bottom currents then probably removed the surficial fine grain-size fraction, leaving rough surface textures of the cones, which backscatter sonar signals strongly in the data recorded here. However, a young cone investigated in detail is characterized by a smooth surface, a marked increase of internal stratification with increasing distance from the summit and upwards concave flanks. Others exhibit central craters, suggesting an explosive than an effusive evolution of these structures. The morphological characteristics of these submarine cones show that they have similar sizes and shapes to cinder cones onshore São Miguel.

1. Introduction

The Terceira Rift is located in the middle of the Atlantic Ocean roughly 1500 km west of continental Portugal. It is defined by a succession of deep transtensional rift basins and bathymetric highs of volcanic origin, which are distributed along the westernmost tip of the Eurasian–African plate boundary (Fig. 1a/b). Few of the bathymetric highs pierce the sea surface, representing the islands of São Miguel and the Formigas islets in the southeastern domain of the Terceira Rift (Fig. 1c). Therefore, this area offers unique study conditions for submarine volcanism encompassing a wide range of water depths from shallow to more than 3000 m, which implies a strong diversity of eruption conditions. For example, volcanism close to the sea surface causes steam driven explosions (phreatomagmatism) forming tuff rings. This type of volcanism is called Surtseyan named after the island of Surtsey off the southern coast of Iceland (e.g. Moore, 1985). Such tuff rings are also described in the Azores region, e.g. the Capelas tuff cone at São Miguel (Solgevik et al., 2007) or Capelinhos at Faial (Cole et al., 2001). In water depths of a few 100 m, the effect of sea water boiling predominates (instead of vaporization; Moore, 1985) and the eruption column is concentrated within the submarine domain interacting with surface currents and the sea surface (Cashman and Fiske, 1991). Since every 100 m of water depth corresponds to an increase of pressure by 1 MPa (10 bar), exsolution and expansion of magmatic volatiles – which force explosions at water depths of several hundred meters – are reduced in deeper domains (White et al., 2015). Hence a critical depth has been assumed in the past, below which explosive volcanism is not possible and an effusive type of volcanism (e.g. pillow lavas) is expected only. However, observed deep sea deposits contradict this assumption (e.g. Hekinian et al., 2000).

The submarine domain of the Azores is dominated by several linear volcanic ridges, a very common geomorphological feature in extensional settings like e.g. the Mid-Atlantic Ridge (e.g. Smith and Cann, 1999; Tempera et al., 2013). They are characterized by heights of >1500 m and built up by individual lava terraces, fissure eruption deposits as

* Corresponding author. Tel.: +49 40 42838 6369; fax: +49 40 42838 5441.
E-mail address: benedikt.weiss@zmaw.de (B.J. Weiß).

http://dx.doi.org/10.1016/j.jvolgeores.2015.07.028
0377-0273/

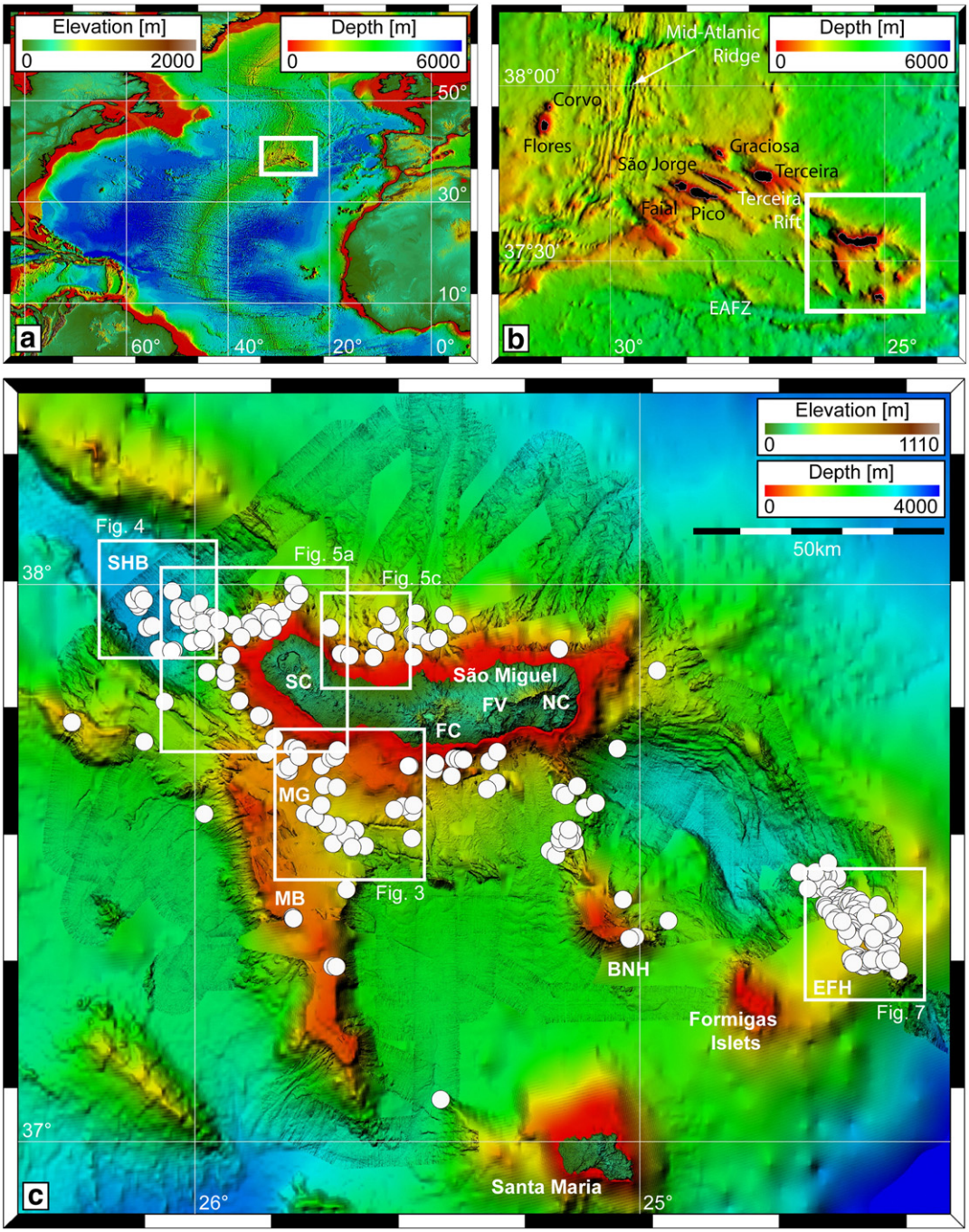

Fig. 1. Bathymetric map of the working area. Location of the Azores (a) and the distribution of the islands within the Azores archipelago (b). White dots mark mapped volcanic cones in the working area (c). Lighting from Az320°/Alt70°. EAFZ: East Azores Fracture Zone. Volcanos: SC: Sete Cidades Volcano; FC: Fogo Volcano Complex; FV: Furnas Volcano; NC: Nordeste Complex. SHB: South-Hirondelle-Basin; MG: Monaco Graben; MB: Monaco Bank; BNH: Big North High; EFH: East Formigas High.
Background bathymetric data is from Lourenço et al. (1998) and ETOPO (Amante and Eakins, 2009). Topographic data is from ASTER GDEM.

well as small volcanic cones with diameters <3000 m. These kinds of cones have been described by several authors e.g. in the case of the Azores region (Stretch et al., 2006; Mitchell et al., 2012; Casalbore et al., 2015), the Mid-Atlantic Ridge (Smith et al., 1995a), the Reykjanes Ridge south of Island (Magde and Smith, 1995; Smith et al., 1995b) and the Puna Ridge, Hawaii (Smith and Cann, 1999), all of them based on bathymetric, backscatter and/or side-scan data only.

In contrast, in this study we present the first combined analysis of hydroacoustic (bathymetry and backscatter data) and high resolution multi-channel seismic data in the Azores domain focusing on submarine volcanic structures. 252 volcanic cones were observed in the southeastern Terceira Rift, mainly concentrated in the vicinity of São Miguel Island and northeast of the Formigas Islets (Fig. 1c). 39 of them are covered by seismic data, although not all of them have been crossed centrally. Most of the cones were assigned to one of three different geographical domains. The cones within each domain were characterized in terms of topographic characteristics, backscatter facies and seismic image (as far as available) before a general statistical overview of the topographic properties like water depth, width, height and slope angle will be given. Finally, the evolution of the cones, the surface texture

and its implication as well as the different geological settings will be discussed.

2. Regional setting

The Terceira Rift is the Eurasian–Nubian plate boundary with a WSW–ENE directed extension of 4 mm/a (Fernandes et al., 2006). It is located at the northeastern rim of the Azores Plateau, an area where the seafloor is abnormally elevated and roughly defined by the 2000 m contour line (Fig. 1b). West of Faial and Graciosa Island, the Terceira Rift merges with the Mid-Atlantic Ridge (MAR) forming the diffuse Azores Triple Junction (Marques et al., 2013, 2014; Miranda et al., 2014). To the south, the East Azores Fracture Zone (EAFZ) forms the southern rim of the Azores Plateau representing the fossil trace of the Eurasian–Nubian plate boundary (Krause and Watkins, 1970; McKenzie, 1972; Searle, 1980; Luis and Miranda, 2008). During northward migration of the triple junction, the accretion of large volumes of extrusives and intrusives as well as underplated material (Luis et al., 1998; Cannat et al., 1999; Gente et al., 2003) caused the creation of thickened crust (Luis and Neves, 2006; Dias et al., 2007; Georgen and Sankar, 2010; Silveira et al., 2010) resulting in the abnormal elevated seafloor of the Azores Plateau.

Recent studies suggest the initiation of the evolution of the plateau and the Terceira Rift to be strongly controlled by rigid response of the lithosphere to changes in the regional stress field induced by tectonic plate kinematics (Lourenço et al., 1998; Miranda et al., 1998; Luis and Miranda, 2008; Navarro et al., 2009; Neves et al., 2013; Weiß et al., 2015). Additionally, the existence of a hot spot (Schilling, 1975; Cannat et al., 1999; Escartín et al., 2001; Gente et al., 2003; Yang et al., 2006) interacting with the MAR or a melting anomaly (Bonatti, 1990; Beier et al., 2008; Métrich et al., 2014) due to an abnormal high volatile content in the mantle (wet spot) may explain the strong volcanism, which has formed the Azores Plateau, the volcanic islands of the Azores Archipelago and submarine linear volcanic ridges.

Several submarine ridges in the Azores have been studied in detail (Mitchell et al., accepted for publication and references therein), e.g. the Condor Seamount west of Faial (Tempera et al., 2013) and a volcanic ridge southeast of Pico (Stretch et al., 2006; Mitchell et al., 2012). They evolved on top of a system of fissures caused by lithospheric extension along the ridge axis. Ridge volcanism is associated with basaltic magma forming a wide range of different volcanic features such as magma terraces, solidified lava flows, crater and collapse structures, linear volcanic chains as well as isolated small circular volcanic cones. These cones are typically characterized by diameters of 300 m to 3000 m and slope angles of roughly 15° to 25°. Photos taken from similar cones e.g. on top of the median ridge of the Mid-Atlantic Ridge near 34°50′N (south of the Azores Plateau) show hyaloclastites and pyroclastic deposits of unsorted irregularly fragmented rocks (Hekinian et al., 2000), which suggests that the magma was disaggregated during explosive eruptions. Since cones on the submarine Pico Ridge, in contrast, show both smooth as well as rough surface textures in backscatter data, some authors suggest different eruption rates and/or effusive as being responsible for the different surface properties (e.g. Stretch et al., 2006).

In the southeastern domain of the Terceira Rift, three large subaerial active volcanoes are located at São Miguel Island (Fig. 1c). From west to east, these volcanoes are the trachyte stratovolcano of Sete Cidades Volcano, the trachyte Fogo Volcano Complex (also known as Água de Pau) and the trachyte Furnas Volcano (Wood, 1980; Moore, 1990; Moore and Rubin, 1991). The youngest and smallest one, Furnas, started to evolve about 100 ka ago (e.g. Moore, 1990) and overlies the remnant Nordeste Volcano Complex, which shows reliable ages of maximum 0.8–0.9 Ma (Johnson et al., 1998; Sibrant et al., 2015). Formation of Fogo and Sete Cidades started about 200 ka (e.g. Moore, 1990). In between these active main volcanoes, fields of alkali basalt lava flows and cinder cones are situated revealing Upper Pleistocene and Holocene ages. Cinder cones usually form during monogenetic explosive eruptions (Schmincke, 2005) and resemble submarine volcanic cones in size and shape.

3. Data and methods

This work is based on high resolution bathymetric, backscatter and multichannel seismic data collected by University of Hamburg scientists on board of *RV Meteor* during cruise M79/2 in 2009 (Hübscher, 2013). For the bathymetric and backscatter data measurements the Kongsberg EM120 and EM710 multibeam echosounders installed on board were used. These systems emit 12 kHz and 70–100 kHz acoustic signals, respectively, and soundings from the backscattered signals were recorded over approximately four times water depth over an area elongated perpendicular to the vessel track. Both, travel time and backscattered energy per signal are recorded in fixed receiver beams of known geometry. Based on velocity information of the water column and the travel time, water depth is calculated. The amount of backscattered energy depends on the seafloor's roughness — the rougher the seafloor, the higher the backscattered energy is (black in the backscatter maps presented here). During processing, segments lacking navigation due to errors were filled with interpolated positions, depth information was corrected based on revised water velocity profiles and each recorded beam was edited to eliminate spikes. Grid node spacing was mostly chosen as 30 × 30 m, but smaller spacings were chosen for detailed views as mentioned in figure captions. However, as the sonar acoustic footprint is equal to ~2% of water depth, effective resolution can be less than the grid spacing. To fill areas where we had not surveyed, a background bathymetric map was created from data of a 1 × 1 km grid presented by Lourenço et al. (1998), which can be found under http://w3.ualg.pt/~jluis/acores_plateau.htm, and ETOPO1 data (~1.9 × 1.9 km) published by Amante and Eakins (2009). The onshore topographic data shown is originated from the ASTER GDEM, which is a product of METI and NASA. It contains a 1 arc sec (30 m) grid of elevation postings. For visualization purposes the different data sets have been imported to an ArcGIS 9.3 system. Using this system as well as the QPS Fledermaus 3D software high resolution bathymetric data were screened for topographic positive structures with a maximum width of 5 km. To distinguish between volcanic cones and potential blocks of debris avalanches only structures with a circular to oval shape in plan view and a domed vertical profile have been mapped. Each mapped structure were characterized by the following properties: (1) water depth of the summit; (2) basal diameter measured orthogonal to the gradient of the submarine slope the cone lies on; (3) height given as elevation difference of summit and interpolated seafloor below; and (4) slope angle calculated from the arc tangent of height and half basal diameter.

39 cones are covered by high resolution 2D multichannel seismic data. The corresponding seismic signals were generated by two clustered GI-Guns with a generator volume of 45 cubic inch and an injector volume of 105 cubic inch each. For data recording a 600 m long asymmetric digital streamer was used, containing 144 channels with an average spacing of 4.2 m. Shots were fired every 25 m at a speed of 5 kn. Data processing involved trace editing and CMP sorting with a CMP increment of 5 m as well as the application of several bandpasses with 10/20/300/400 Hz, a spike & noise burst filter and a FK-filter (e.g. Hübscher and Gohl, 2014). Finally, NMO-correction, stacking and a post stack time migration has been performed. For the detailed studies of one volcanic cone (Fig. 6) 144 channels were first stacked so that they formed a group of 96 effective channels with a regular spacing of 6.25 m. This data has been filtered by a bandpass of 10/15/150/300 Hz, CMP increment has been decreased to 3.125 m and NMO-correction has been applied based on picked velocity profiles.

4. Observations & interpretation

The cones were grouped into different categories according to their location (Fig. 2). One category is orientated along faults and bathymetric

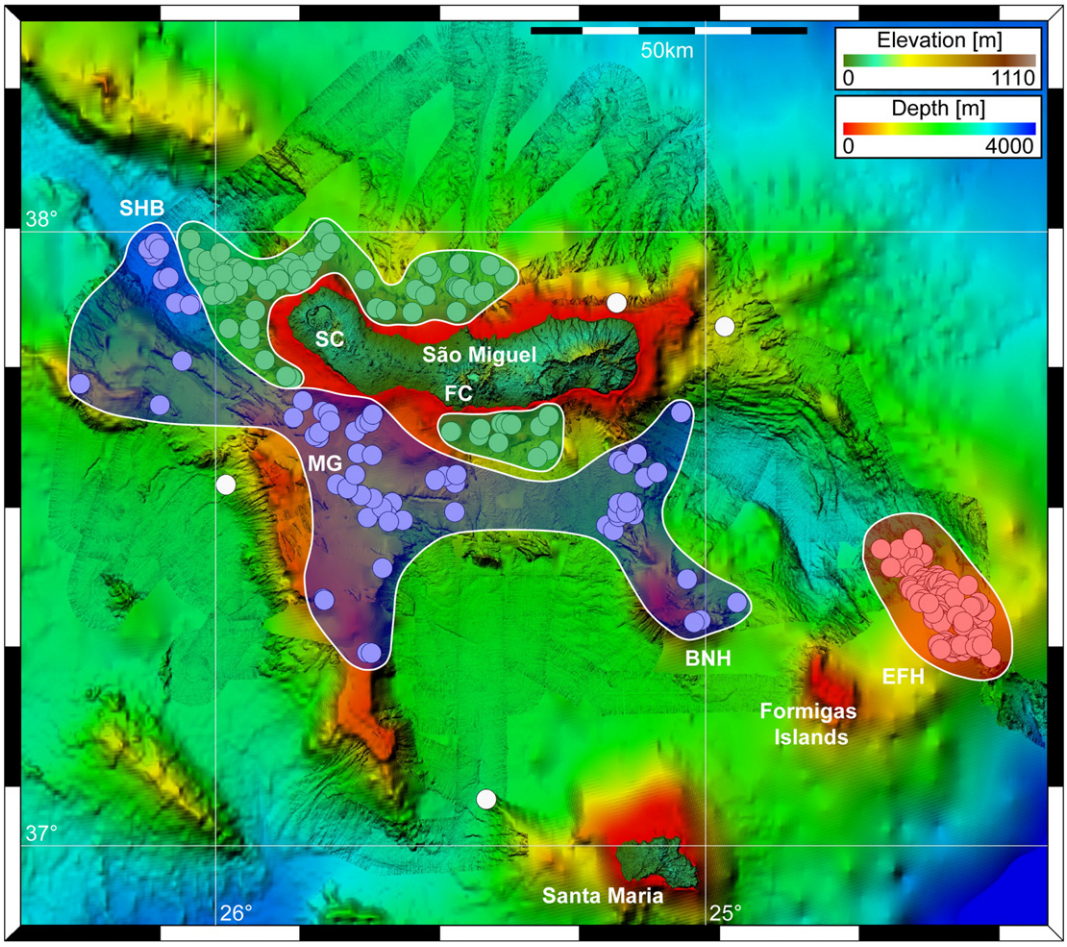

Fig. 2. Categories of submarine volcanism according to location. Blue: Volcanism along structural lineaments; green: volcanism at the submarine domain of Sete Cidades and Fogo; red: volcanism at East-Formigas High. Lighting from Az320°/Alt70°. Volcanos: SC: Sete Cidades Volcano; FC: Fogo Volcano Complex. SHB: South-Hirondelle-Basin; MG: Monaco Graben; BNH: Big North High; EFH: East Formigas High.

lineaments (blue area in Fig. 2). A second group was chosen around the submarine flanks of Sete Cidades Volcano as well as north and south of the Fogo Volcano Complex (green area in Fig. 2). Further cones cluster on top of East Formigas High where the density of cones is highest in the working area (red area in Fig. 2), which was chosen as a third group. Each of these categories represents a specific volcanic setting controlled by distinct volcanic mechanisms. Below, they will be presented in detail.

4.1. Volcanism along structural lineaments

South of São Miguel Island, many volcanic cones are either distributed along faults and magmatic lineaments or form volcanic chains (blue area in Fig. 2). Most cones are located in the vicinity of Big North High and in the Monaco Graben in water depths of 400 m to 2000 m (Fig. 3a–d). A further cluster of aligned cones is within the South-Hirondelle Basin where water depth reaches 3200 m (Fig. 4a–c). In the backscatter data (Figs. 3d, 4c), the cones appear as circular to elongated structures which most of them differ from their surroundings by a higher backscatter (rougher surface). Furthermore, two cones in the South-Hirondelle Basin are located on top of a small area producing high acoustic backscatter, which is also recognizable in the bathymetry (marked with purple arrow in Fig. 4b–c).

Cones in the Monaco Graben reveal a transparent and occasionally layered seismic reflection pattern. As illustrated by the two cones in Fig. 3a and b, all cones crossed with seismic lines within the graben terminate on the same reflection horizon, which is also a prominent boundary between mainly (sub-) parallel to divergent reflections onlapping each cone's flanks and a sub-parallel, contorted and tilted reflection pattern below. Underneath, a strong amplitude reflection marks the transition to the acoustic basement and the corresponding area of low seismic penetration. Both, basement and overlaying unit are disrupted by faults, but none of them penetrating the seafloor. Faults below the cones are not clearly observable, though tilted and offset reflections suggest their presence.

Following Weiß et al. (2015) we interpret the acoustic basement as the volcanic basement, which has been offset during the formation of the Monaco Graben. Faults active during extension thus partly acted as magmatic pathways controlling the distribution of the cones within the graben. Therefore, the unit overlaying the acoustic basement represents the corresponding syn-rift deposits. Since the flanks of the cones terminate on top of this unit and the reflection of the uppermost unit onlap these flanks, the cones were active during the end of graben formation. This agrees with the lack of seismicity in this region (Weiß et al., 2015), indicating that there is neither recent extension nor recent magmatic ascent taking place. The uppermost unit reflects current controlled sedimentation conditions during tectonic quiescence. It forms mounded elongated patch drifts and associated moats, flanking the cones where the bottom currents are intensified (Fig. 3a/b).

Cones in the South-Hirondelle Basin have not been directly crossed by seismic data, but an area with a remarkably rough surface is covered by seismic data. It is characterized by strong chaotic and disrupted reflections indicating a volcanic origin (purple arrow in Fig. 4a). Since the high acoustic impedance of this area hampers seismic imaging of

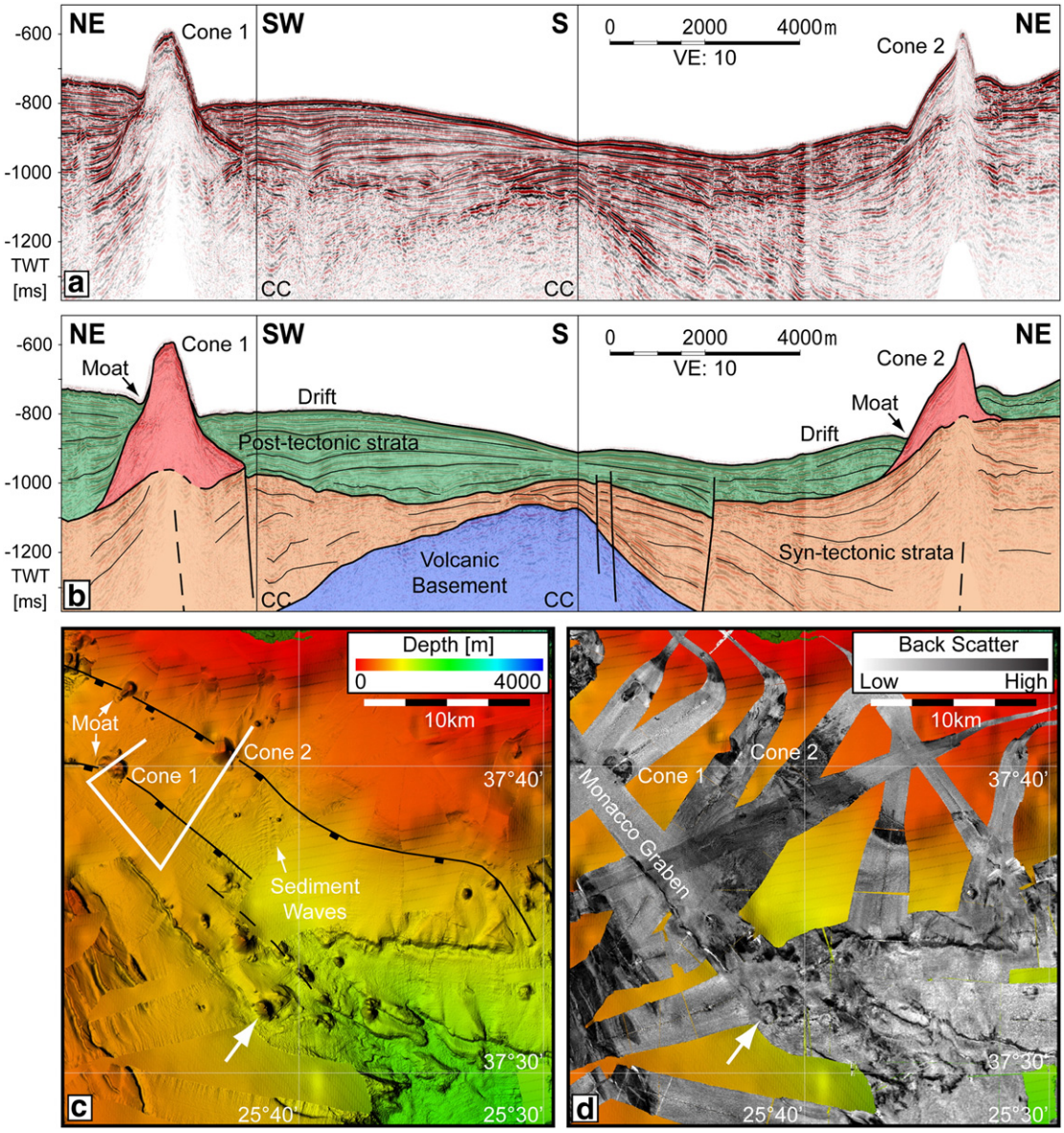

Fig. 3. Fault controlled volcanism. Seismic section (a), its interpretation (b), bathymetric (c) and backscatter data (d). Black vertical lines in (a, b) indicate the course changes (CC), white line in (c) shows the location of the profile. White arrows in (c) and (d) indicate the cones with a crater. For detailed location of (c) and (d) see Fig. 1. Lighting from Az270°/Alt70°. VE: vertical exaggeration.
Normal faults (black) and volcanic lineaments (black dashed line) in (c) after Weiß et al. (2015).

deeper structures, the existence of a fault plane beneath this structure remains uncertain. Nevertheless, the shape and orientation of the high backscattering area and the strike direction of the corresponding volcanic lineament parallel to the southwestern one support this interpretation. Therefore, the northeastern volcanic lineament is interpreted as being located on top of a small volcanic plateau which has been formed during effusive fissure eruptions. In contrast, the southwestern volcanic lineament clearly correlates with the prominent normal fault identifiable in the seismic data (red arrow in Fig. 4).

4.2. Parasitic volcanism

Cones assigned to this category occur on the submarine flank of Sete Cidades Volcano as well as north and south of the Fogo Volcano Complex (Fig. 5a–d). They comprise the largest cones which have been measured in the working area, with diameters of 1500 m or more. Examples are the northernmost cone north of Fogo (marked with a black arrow in Fig. 5c) and a cone southeast of Sete Cidades (also marked with a black arrow in Fig. 5a) described in detail later on (Fig. 6). The water depth commonly ranges from 400 m to 1200 m but reaches maximum values of 3200 m west of Sete Cidades Volcano, where its flank extends down to the South-Hirondelle Basin floor. Most of the cones are distributed without any obvious pattern or organization. Solely on the northwestern flank of Sete Cidades Volcano (Fig. 5a), cones group along faults crosscutting the northeastern margin of the South-Hirondelle Basin and continuing across the main body of Sete Cidades Volcano and the western island of São Miguel, respectively (Weiß et al., 2015, and references therein). The seafloor in the Sete Cidades domain produces high backscattering amplitudes and hence appears to be rough before it reaches the South-Hirondelle Basin floor characterized by a smooth sediment surface (Fig. 5b). Since the contrast in roughness between most of the cones and the surrounding seafloor is low, it is difficult to identify cones based on backscatter data information only. Nonetheless, a few cones are present, which are characterized by gray in Fig. 5b and therefore suggesting smooth surfaces. Examples are the cone southwest of Sete Cidades crossed by seismic reflection data and a cone northwest

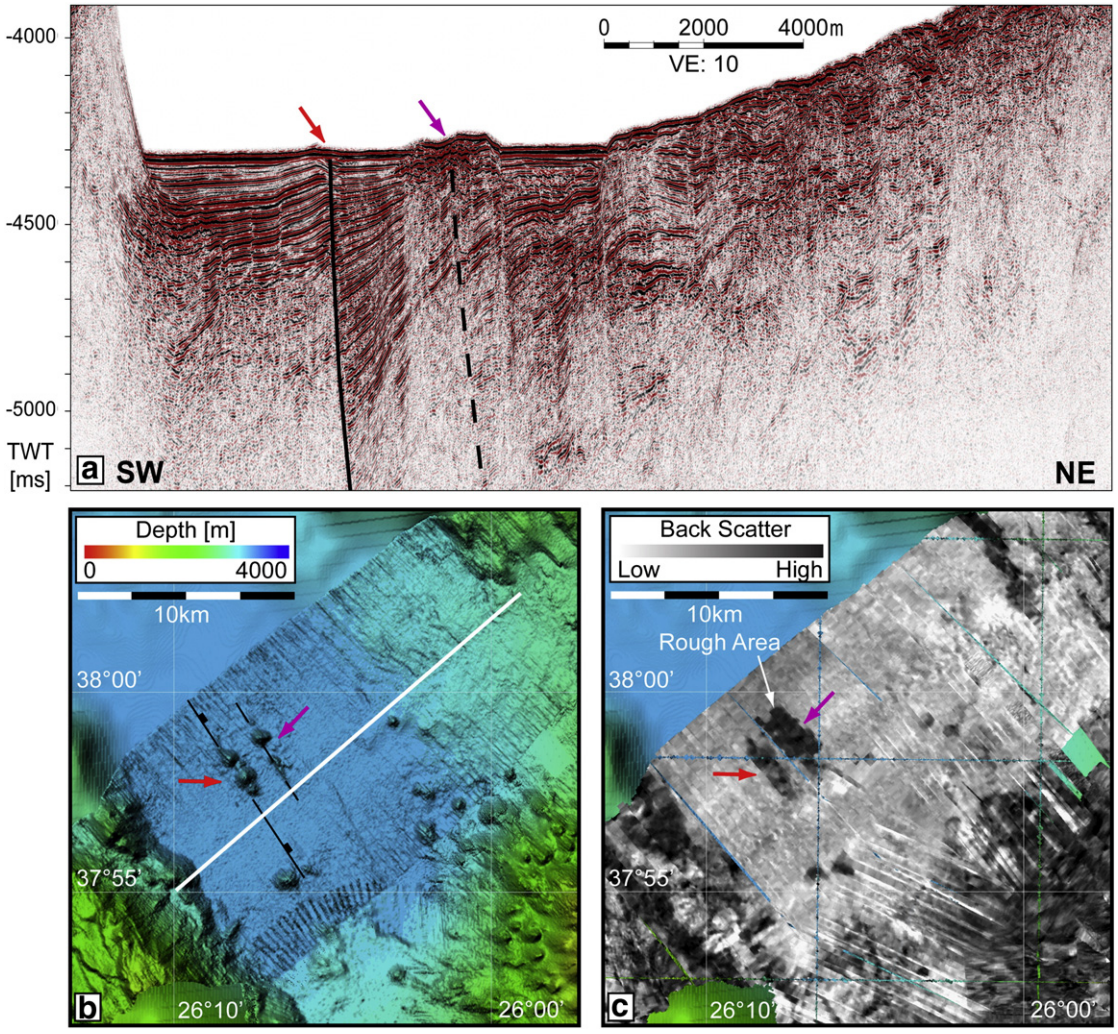

Fig. 4. Fault controlled volcanism in the deep areas. Seismic section (a), bathymetric (b) and backscatter data (c). White line in (b) shows the location of the profile. Colored arrows trace the two volcanic lineaments in the deep sea domain of the South-Hirondelle Basin. For detailed location of (b) and (c) see Fig. 1. Lighting from Az320°/Alt70°. Grid spacing in (b, c) 40 × 40 m. VE: vertical exaggeration.
Normal (black) and inferred (black dashed line) faults in (b) after Weiß et al. (2015).

of that edifice with a small summit crater (both marked with B in Fig. 5a/b). Aside from the second mentioned cone, two collapsed cones are observable. In each case, a new cone has grown up within the collapse structure (marked with C in Fig. 5a/b). In contrast to the submarine flank of Sete Cidades, the northern flank of São Miguel between the Sete Cidades and Fogo domain (Fig. 5c/d) is generally characterized by a brighter backscatter facies and a smooth seafloor, respectively. Volcanic cones commonly appear as black anomalies, but also cones defined by a smooth surface are observable.

On possible reason for the highly backscattering Sete Cidades could be the steep slope (>10°) of this area, which may impede sediment deposition. In contrast, north of the Fogo Volcano Complex a lower slope angle (<6°) allows sediment bodies to accumulate, covering most of the volcanic effusive and explosive.

South of Sete Cidades Volcano, a cone showing a low backscattering surface has been covered by a flank-parallel and a flank-perpendicular seismic line (Fig. 6a–d), the latter one also covering an adjacent cone. They are located on top of a seismic unit revealing distorted and chaotic reflections. Internally, the cones are mostly seismically transparent in the proximal region, but showing few reflections. Distally, internal stratification increases and the slope is concave (Fig. 6a/b). In the transition to the nearby cones, volcanic deposit interfinger (Fig. 6c/d).

Both cones overlie the southern flank of São Miguel Island, where the substrate presumably consists of successions of coarse rock sediments, lava flows and volcaniclastics deposited during the formation of Sete Cidades Volcano. The concave shape of the slope and the arrangement of internal stratification of the cones indicate deposits with a distally decreasing grain size. We therefore interpret the distal domain of the cone as comprising disaggregated volcaniclastic material. Interfingered reflections then represent multiple eruption phases or overlapping depositions of explosive and effusive volcanic material. Since the deposits of the adjacent cone interfinger, the two cones emerged synchronously, but their corresponding eruption phases alternated in time.

4.3. Volcanism at East-Formigas High

More than hundred volcanic cones have been picked on top of the East-Formigas High (Fig. 7a–d). They are distributed in water depths of 200 m to 2000 m. The shallowest point in this region is the crater rim of a cone rising up to a minimum water depth of 110 m (Fig. 7c). This one and two adjacent cones clearly show evidence of summit craters. Again, the locations of the cones do not follow organized patterns, such as would occur if erupted above faults. Nevertheless, faults are present and crosscut the entire East-Formigas High. Into shallow

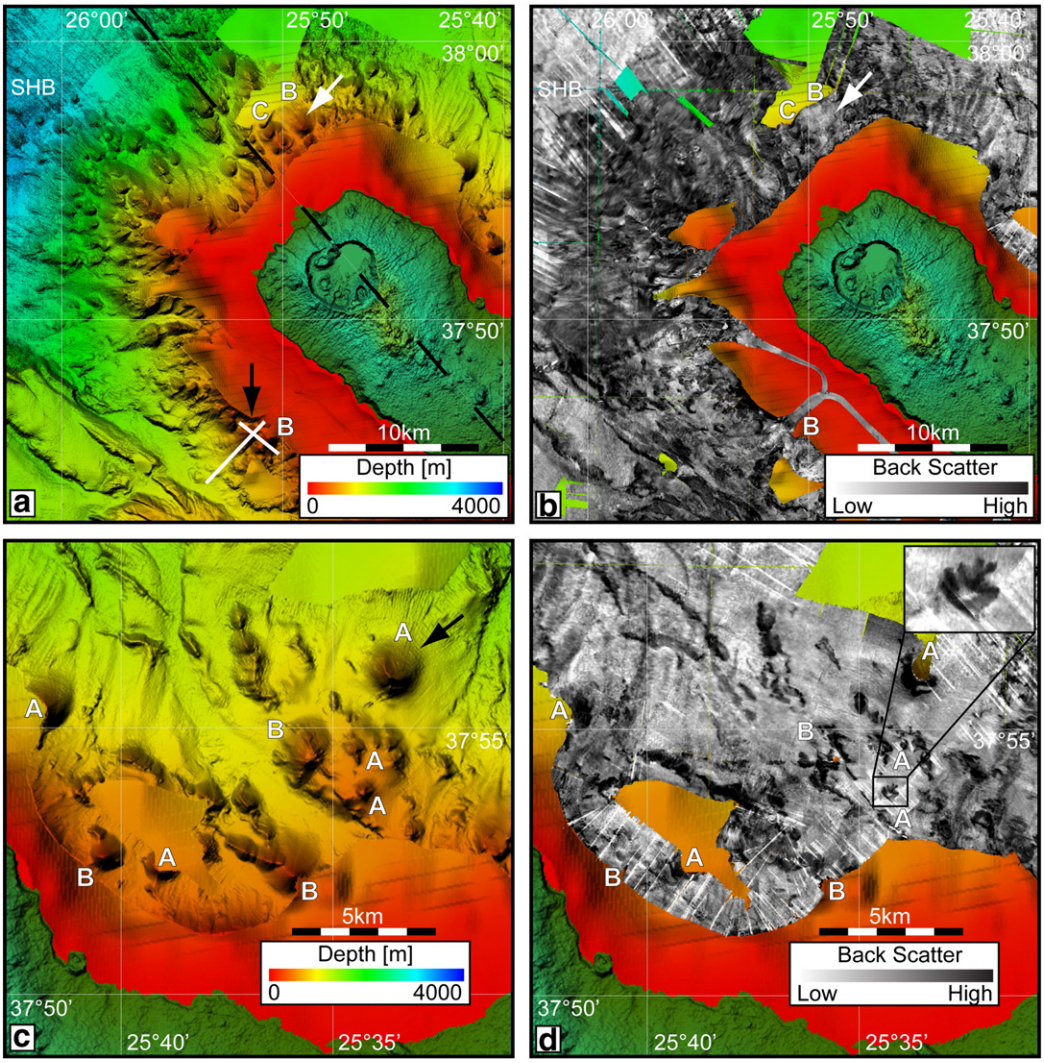

Fig. 5. Parasitic volcanism. The submarine flank of Sete Cidades Volcano is covered with numerous volcanic cones (a). Cones as well as the adjacent seafloor show a dark backscatter facies (rough surface) (b). In contrast, the seafloor north of Fogo Volcano Complex (c, d) is much brighter (smoother), but most cones keep their dark backscatter characteristics (marked with A). Few of the cones in (b) and (d), however, show a bright backscatter facies/smooth surface (marked with B). This category of cones reveals the largest structures mapped in the working area (black arrow in a, c). White arrow in (a) and (b) indicate a cone with a crater. For detailed location see Fig. 1. C: collapse structure and cone within; SHB: South-Hirondelle Basin; white lines in (a): seismic profiles presented in Fig. 6; dashed black line in (a): simplification of the South-Hirondelle Basin margin faults and their onshore continuation after Weiß et al. (2015). Lighting from Az320°/Alt70°.

water, the seafloor shows higher acoustic backscattering. Thus, the identification of volcanic cones purely based on backscatter data becomes less straightforward, since many of them show a rough surface as well. A special case is the shallowest cone (Fig. 7d) which indeed does not show a significantly brighter backscatter facies than the surrounding seafloor, although it lacks a distinct cone–seafloor boundary. For that cone, only the crater rim appears as a well-defined structure.

4.4. Cone morphometrical characteristics and depths

In total, 252 submarine volcanic cones could be identified in the area covered by our high-resolution multibeam data (Fig. 1c). The mapped summits are distributed in water depths from 110 m on top of East Formigas High down to 3200 m in the South-Hirondelle Basin. One of the largest cones is located at the southwestern submarine flank of Sete Cidades Volcano (previously presented in Section 4.2). It shows a diameter of 3000 m, a height of 500 m and a water depth of its summit of 265 m. In contrast, one of the smallest structures which could be identified as a volcanic cone is located on top of Monaco Bank in a water depth of 485 m. It is 110 m in diameter and 14 m high. The average width of all measured cones is 743 m with a standard deviation of 405 m, the average height is (139 ± 77) m with an average slope angle of (20 ± 4)° and they are located in water depths of (1023 ± 705) m. In comparison, cones observed onshore São Miguel – in particular between Sete Cidades Volcano and the Fogo Volcano Complex – are smaller. They have an average width of (484 ± 215) m, a height of (73 ± 36) m and show slightly lower slope angles of (17 ± 4)°.

Fig. 8a shows the distribution plot of size over depth. Water depths of the cones are assigned to ten 300 m bins. Corresponding average diameter and standard deviation per bin are indicated by circles and vertical lines, respectively. One can notice that the average cone width is not a function of the water depth but alternates around an average of 743 m. In contrast, the standard deviation tends to decrease with increasing water depth, declining from 520 m to 70 m (only one cone lies within the 2400 m bin so no standard deviation is given there), before increasing again at 3000 m depth. These cones, which are all located on the floor of the South-Hirondelle Basin, show again an increased variation in size of 250 m. The total number of cones per 100 m depth bin as well as number of cones of a distinct diameter (100 m bin) and height (25 m bins) are presented in Fig. 8b–d. The cone width distribution,

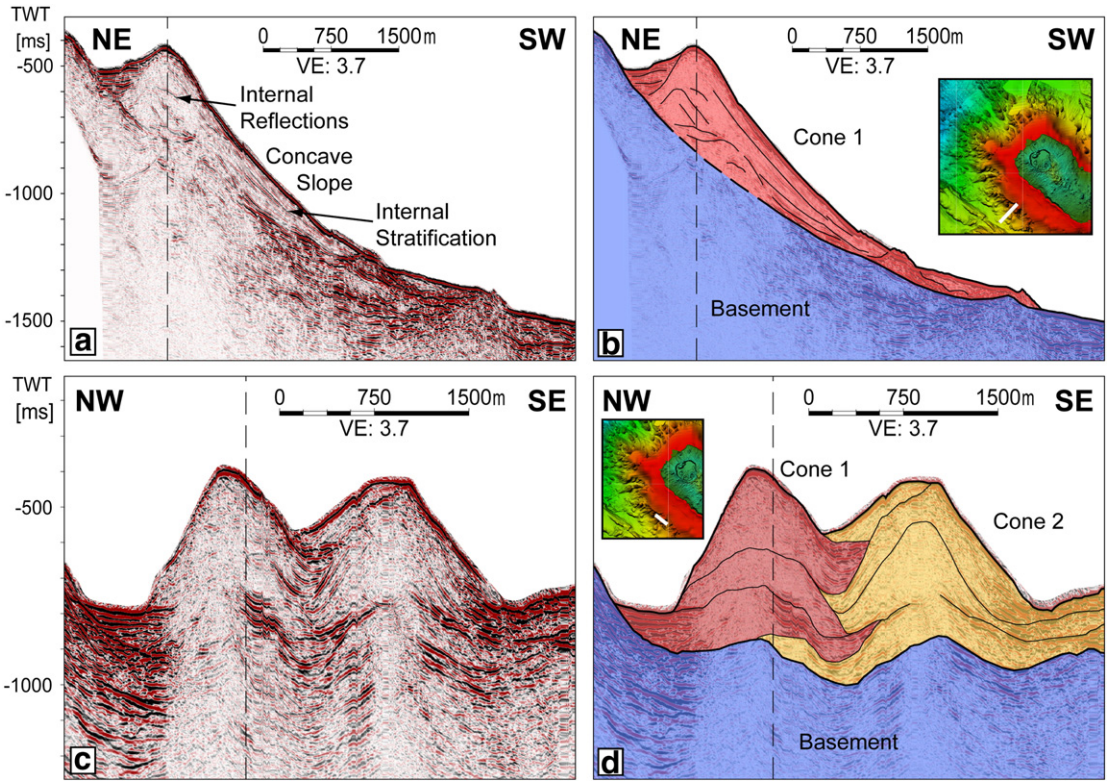

Fig. 6. Parasitic volcanism. Seismic sections (a, c) and corresponding interpretation (b, d). Note the concave shape of the flank and the distal increasing stratification of cone 1 illustrating its explosive nature (b). Depositions of cone 1 and 2 interfinger indicating a synchronous evolution (d). For location of profiles see inset or Fig. 5a. Dashed black vertical lines indicate the intersection of profiles. VE: vertical exaggeration.

when considering cones with a minimum width of 600 m and bins with more than 4 counts (less is expected not to be statistically relevant) only, shows an exponential decrease of cone numbers with increasing size (Fig. 8c, inset). The inverse exponential coefficient of the exponential regression line (red dotted line) is 480 m. Both distribution and exponential coefficient are in a good agreement with observations at and close to the MAR south of the Azores as well as south of Iceland (Smith, 1996). In Fig. 9a the relation between cone heights and cone widths (H/W ratio) is presented. With one exception, all cones are characterized by slope angles lower than the angle of repose of granular material, expected to be 30°. For comparison, the H/W values of cinder cones onshore São Miguel also have been included. Measurements were taken in the same way as for the offshore domain but were based on ASTER GDEM topographic data. It becomes obvious that the onshore cones are smaller and that they tend to reveal lower slope angles than the offshore structures. The ratio of cone height and width plotted against water depth shows that for the offshore cones there is no correlation between cone shape and the water depth of the summits below 300–400 m (Fig. 9b). Above this level, cones tend to be flatter as indicated by the black dashed line.

Most of the submarine cones in the working area have a peaked summit and less of 4% reveal an identifiable crater. This is similar to the onshore cones, but craters of various sizes are much more common here. However, the lack of craters – especially in the deep sea domain – could rather be a problem of horizontal resolution than reality (effective resolution after processing and gridding is e.g. ~75 m in a depth of 3000 m or ~25 m in a depth of 1000 m).

The backscatter data suggests a little majority of cones characterized by high acoustic backscattering (111 of 252), appearing as dark spots like in the Monaco Graben (upper left part of Fig. 3d) and the South-Hirondelle Basin (Fig. 4c) or as an intensely dark speckled area (e.g. marked with A in Fig. 5d). In contrast, 100 of 252 cones show an overall bright backscatter facies (marked with B in Fig. 5b/d). But apart from the backscatter characteristics, both types of cones do not remarkably differ in their topographic characteristics (width, height, slope angle). However, several cones could not reliably be assigned to one of the two categories (41 of 252) since they partially show both low and high backscattered energy or due to their location in an overall "darker" setting, where the contrast between a cone and its surroundings is generally low (Figs. 5b/7b).

5. Discussion

5.1. Explosive or effusive evolution of volcanic cones?

Several observations allow concluding on possible information on the eruption process. Even if several cones include or overprint elongated structures (e.g. Fig. 5c), the cones are predominantly circular and tapered (Figs. 3–7), which reminiscent of a sandheap. This pattern indicates that the deposits of the cones originate from a central vent (which is sometimes part of a volcanic fissure system).

An almost transparent reflection pattern partially revealing some weak internal stratification within the proximal domain of a cone (Fig. 6a) indicates clastic but irregular and unsorted deposits, which are deposited close to their origin, possibly revealing minor effusive/intrusive. In contrast, stratification is clearly observable in the distal domain. Hence, we conclude on an outwards fining sediment composition which was farther distributed by the water column before it settled down. Deposits which mainly have been formed by runout of particles or, in particular, by disaggregation of downslope lava flows producing breccias (Sansone and Smith, 2006) would result in a more irregular to chaotic reflection pattern and, hence, are unlikely. Anyway, reflection pattern rules out a composition of effusive (Hübscher et al., 2015), even if a minor presence cannot generally be excluded (e.g. Fig. 5d, inset).

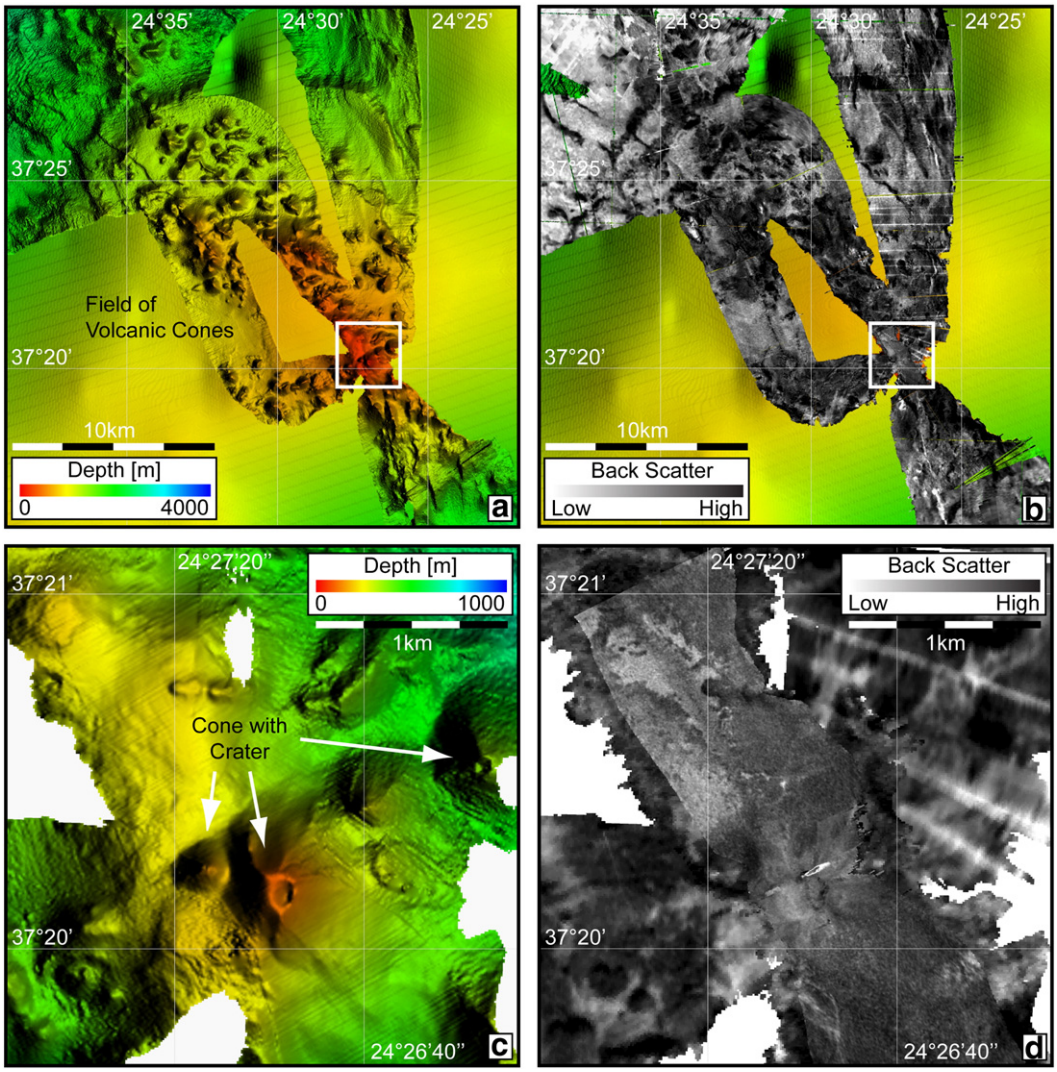

Fig. 7. Constructive volcanism. Bathymetric (a, c) and backscatter data (b, d). White boxes in (a) and (b) indicate the location of blow-ups in (c) and (d), respectively. The East-Formigas High is covered with many volcanic cones (a) and several revealing craters (c). In general, this area is characterized by rough surface (high backscattered energy) and roughness of volcanic cones does not strongly differ from their surroundings. For detailed location see Fig. 1. Lighting from Az90°/Alt70°. Grid spacing in (c, d) 10 × 10 m.

Few cones show summit craters (Figs. 3c, 5a and 7c). Generally, such craters may result from explosions or collapses. Onshore, craters at volcanoes similar in size (cinder cones) are commonly the result of explosive eruptions (Wood, 1980; Schmincke, 2005). These volcanoes are formed by monogenetic volcanism resulting from propagation of small batches of magma (Németh et al., 2003). In contrast, pit craters (collapse features) typically occur at much more complex volcanic systems characterized in particular by internal magma reservoirs/flows and rift zones usually causing collapses. Examples for such volcanic systems are e.g. the shield volcanoes of Hawaii (Okubo and Martel, 1998) or the adjacent Lō'ihi Seamount (Garcia et al., 2006). Hence, we suggest that the observed craters were formed by submarine explosive eruptions similar to those studied in detail by e.g. Chadwick et al. (2008).

Based on these interpretations and since the H/W ratio is nearly uniform (implying nearly uniform slope angles) over all mapped cones (Fig. 9a), we conclude on volcaniclastic particles deposited near the angle of repose being the main component of these structures. Associated hyaloclastites and pyroclasts were described e.g. for the East Pacific Rise region (Smith and Batiza, 1989), the Mid-Atlantic Ridge (Hekinian et al., 2000) and the Aegean Sea/Mediterranean (Nomikou et al., 2012). Meyer et al. (1996) observed tuffs, lapilli and pillow breccias at obducted seamounts of similar (estimated) size in the Masirah island ophiolite (Oman) also concluding on explosive eruptions during formation of these cones. In contrast, a remnant seamount in the Troodos ophiolite (Cyprus) consists of pillow lavas and lava tubes, which is flat but still close to the lower limit of the H/W ratios observed in this study (Eddy et al., 1998). However, it is part of a much more complex and wider tectono-magmatic system (including a caldera) and is subaerially exposed since upper Miocene (Robertson, 1998). Hence, erosion may have washed away the unconsolidated volcaniclastics leaving an early effusive core of a larger edifice.

Since the H/W ratio displays no dependency on the water depth below 300–400 m (Fig. 9b), the process of cone formation is assumed not to be controlled by depth or ambient water pressure, respectively. These analogies in the topographic characteristics indicate that there is only one common eruption mechanism driving the genesis of the cones. This is in accordance with other studies conducted in the Azores (Stretch et al., 2006; Mitchell et al., 2012; Tempera et al., 2013; Casalbore et al., 2015), where the same deduction for submarine volcanic cones southeast of Pico, west of Faial and in the vicinity of Terceira Island is drawn, based on bathymetric and side-scan data.

In shallow waters of less than 300–400 m the upper limit of the H/W ratio slightly decreases to a maximal value of 0.21 at 120 m (Fig. 9b) indicating a trend to flatter structures. Corresponding observations at shallow cones in the Pico and Terceira region has also been described

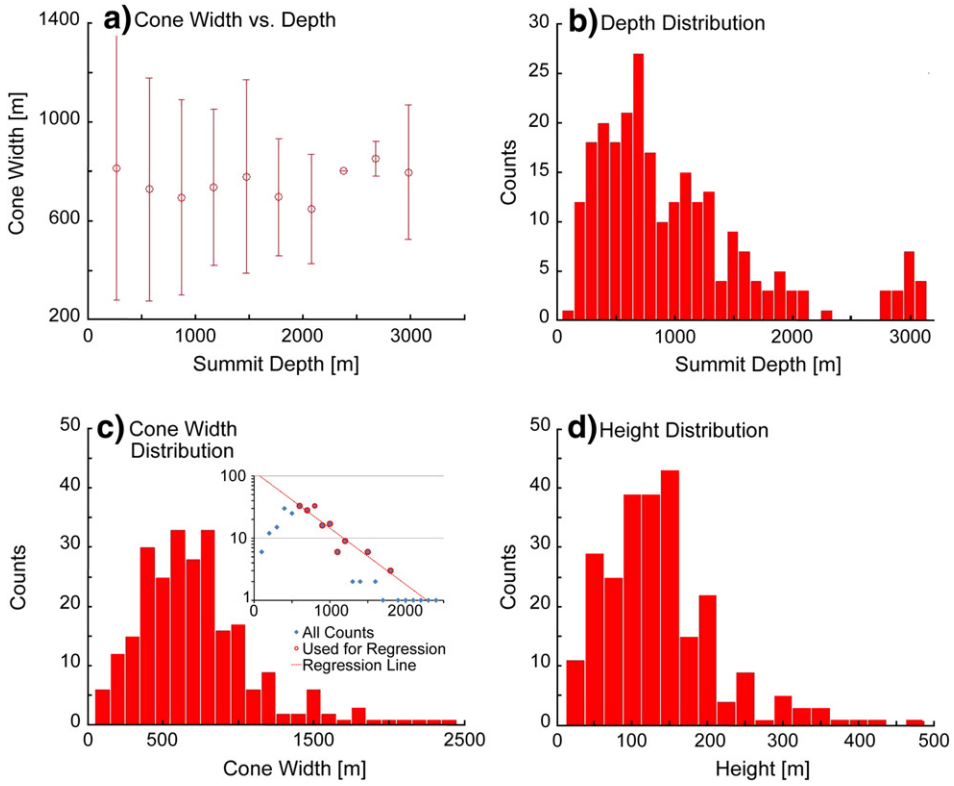

Fig. 8. Cone morphometrical characteristics and depths. Distribution of cone diameters with depth (a). Circles indicate the average and vertical lines the standard deviation of all cones within 300 m water depth bins. Note that the average shows no dependency on water depth, whereas the standard deviation tends to decrease. Total number of cones in a certain water depth (100 m bins, b), with a certain diameter (100 m bins, c) and a certain height (25 m bins, d). Please note that cone size distribution shows an exponential trend when considering cones wider than 500 m and bins with more than 4 counts only (red circles in (c), inset). Blue squares show the original values on a logarithmical scale as also shown by the linear red histogram.

by Mitchell et al. (2012) and Casalbore et al. (2015), respectively. Following Cashman and Fiske (1991), the reduced height is interpreted as the result of eruption columns, which spread along the close sea surface boundary leading to a wider area influenced by volcanic fallout. Therefore, the eruption mechanism in the shallow domain is the same as in deeper waters, but the cone shape is affected by a direct interaction of corresponding submarine explosive eruptions and the water surface. Such eruptions likely produce emissions into the air above the water level, so the inflection point of the upper H/W ratio in depth can be considered as the regional critical water depth above which submarine eruptions pose a hazard potential to people and environment above the sea level (Hübscher et al., 2015). However, this critical water depth is a rough estimation only, since the time of the eruptions and, therefore, the associated sea levels are unknown.

Cones with a diameter of ≤500 m do not follow an exponential size distribution (Fig. 8c, inset), which indicates that there is an additional factor affecting the evolution of small cones. One explanation could be that there is a critical volume of melt needed to be able to reach the seafloor and erupt. Since resolution of our bathymetric data is high enough, an underestimation of these cones appears to be unlikely (Smith, 1996).

In summary, the cones described in this study resemble the cones that have been measured in other regions of the Azores in height and diameter (Stretch et al., 2006; Mitchell et al., 2012; Tempera et al., 2013; Casalbore et al., 2015). Hence, the measured dimension seems to be typical for the Azores Plateau, but has also been reported e.g. from the slow spreading Reykjanes Ridge north and the slow spreading Mid-Atlantic-Ridge at 24°–30°N south of the Azores domain (Magde and Smith, 1995; Smith et al., 1995a,b), the Puna Ridge, Hawaii (Smith and Cann, 1999) as

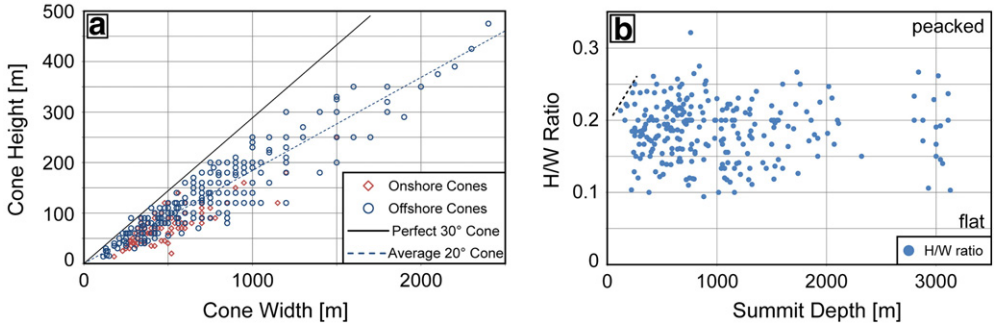

Fig. 9. Relation between cone width and height. Both offshore cones and cones onshore São Miguel are underneath the line describing a perfect cone with 30° slopes (a). Ratio of height and width (H/W) of cones deeper than 300–400 m is independent of the water depth (b). Dotted line in (b) indicates a decrease of the maximal H/W ratio values in shallow water depths (<300–400 m).

well as in the Mediterranean near Santorini/Aegean Sea (Nomikou et al., 2012).

In comparison with the submarine structures, cones onshore São Miguel Island are smaller and show slightly lower slope angles (Fig. 9a). This is relevant to observations on- and offshore Pico (Stretch et al., 2006) and is probably caused by a higher erosion rate in the subaerial domain. But due to the general similarities, we consider the offshore cones to be the submarine equivalent of the onshore cinder cones, which are a typical result of monogenetic alkali-basaltic volcanism on São Miguel Island (Wood, 1980; Moore, 1990; Moore and Rubin, 1991; Schmincke, 2005).

Finally, the question may rise up why less than 4% of the cones show a noticeable crater although they are interpreted as structures with an explosive origin. Possible explanations could be that either the craters in deep water are commonly below resolution as mentioned above, that former craters have been filled up by late eruptional and younger sediments or that the crater rims are often instable and tend to collapse after the eruption cycle has ended (Chadwick et al., 2008; Hübscher et al., 2015).

5.2. Backscatter facies of young and old cones

It is commonly assumed that a smooth or rough texture of submarine lava flows is a relative marker for high or low eruption rates, respectively (e.g. Griffiths and Fink, 1992; Gregg and Fink, 1995; Batiza and White, 2000). According to studies at the Mid-Atlantic-Ridge (Magde and Smith, 1995; Smith et al., 1995a), Stretch et al. (2006) therefore correlated the surface characteristics of the submarine cones near Pico Island with the corresponding magma supply. Hence, the predominance of smooth cones in the Pico area accounts for the hypothesized magma upwelling in the Azores domain. On the contrary, the rough scones (in that study described as hummocky) are supposed to be caused by different eruption styles, lower eruption rates and/or effusive like pillow lavas. Therefore, their reported larger size may result from subsequent lower feeding rate eruptions of primary smooth cones, reflecting a variability of the eruption rate over time. But in contrast to these authors, our measurements did not reveal a majority of smooth cones. Therefore, the increased number of rough cones suggests a minor magma supply in the southeastern Terceira Rift compared with the Pico area. However, the observation of rough cones being systematically larger than smooth cones was not confirmed in this study. Since the cones do not show a difference in the topographic features in general and particularly in size, e.g. a higher content of effusive appears to be more unlikely. Indeed, lobe like features in the foot region of a few cones (e.g. inset of Fig. 5d) indicate effusive eruption phases in between, but we propose the interpretation that the different surface textures do not reflect diversity in the eruption mechanisms.

Due to the following evidence, we rather suggest that a smooth cone corresponds to a young one, whereas matured cones are characterized by a rough surface. (1) All verifiably extinct volcanic cones reveal a dark backscatter facies (as indicated by onlapping sediments on the cone flanks in the Monaco Graben, Fig. 3). (2) The seismically covered cone at the southwestern slope of Sete Cidades is both smooth and young, since it onlaps the slope sediments (Figs. 5b/6). (3) Both smooth and rough cones occur together. The vicinity of recent and long-time extinct structures seems to be more likely than different volcanic mechanisms forming the same kind of topographic structures. (4) The seismic data shows no difference in reflection pattern between cones with the two types of surface. A change in reflection pattern (e.g. resolution of internal structures and transparency) is occasionally dependent on the profile orientation only (e.g. Fig. 6a/c) and can be observed at both smooth and rough cones.

Following this assumption, winnowing as observed by Kokelaar and Durant (1983) is a possible explanation for the increased slope roughness of matured cones. Current controlled sedimentation structures, such as moats (Fig. 3b) and sediment waves (Fig. 3c) e.g. in the Monaco Graben suggest the presence of bottom currents, which may remove the fine grain content of the volcaniclastic sediments exposing bare rocks and effusive over time.

5.3. Submarine volcanic domains

Submarine volcanism producing the described cones clusters in three different domains (Fig. 2), each of them reflecting a specific mechanism of magma supply.

A first category of cones is located on top of faults that represent magma migration pathways (Figs. 3 and 4). Hence, volcanism is most likely controlled by regional tectonics. An example is the Monaco Graben, where the evolution of the volcanic cones is assigned with the graben formation (Weiß et al., 2015; this study, Fig. 3). However, since graben formation and seismicity ceased, no recent volcanism is observable here.

The second category of cones is distributed on top of the submarine flanks of Sete Cidades Volcano and the Fogo Volcano Complex (Fig. 5). Their existence is interpreted as being linked to magmatic processes of the main volcanic bodies and as parasitic structures, respectively. Both dike and fissure related secondary magmatism are probably feeding the submarine cones. Elsewhere, lava tubes or channels have been described feeding submarine effusive eruptions from e.g. onshore magma sources (Smith and Cann, 1999). But since low viscous and degassed magma is necessary for their evolution, it is implausible to assume tubes etc. feeding explosive structures. The absence of these kinds of lava flows is also in agreement with the lack of tumuli structures as observed e.g. around the shelf of Pico (Mitchell et al., 2008).

Finally, a high concentration of cones is found on top of East-Formigas High (Fig. 7). Isolated from subaerial volcanism and not controlled by faults they superimpose a huge magmatic underwater body, which might represent a juvenile formation phase of a subaqueous seamount ultimately resulting in a new volcanic island. Therefore, the magma source of the cones is associated with the growth of the main body. But in contrast to parasitic volcanism, the cones do not represent a secondary feature of a major subaerial volcano as already mentioned. However, it remains unclear if a major volcano will develop later on in the case of subaerial exposure and – as a consequence – if the distributed explosive volcanism is caused e.g. by the enhanced cooling of the surrounding water. An increased seismicity in this region (Weiß et al., 2015) is most likely reflecting both tectonic processes and magma ascent.

5.4. Pyroclastic deep sea volcanism

For a long time, explosive eruptions in the deep sea have been assumed to be unlikely, since the high ambient pressure hampers the dissolution of gas in the magma (e.g. Schmincke, 2005). However, in recent years several studies have been published describing explosion deposits or observations of active pyroclastic activity in maximum water depths of 4000 m (e.g. Davis and Clague, 2006; Sohn et al., 2008; Rubin et al., 2012 and references therein). We therefore contribute to this discussion since the deepest mapped volcanic cone is located at the seafloor in a water depth of 3200 m. Indeed its explosive origin is deduced by its topographic characteristics only. But again, comparing the cones in the submarine domain of Sete Cidades Volcano distributed in water depths of 400 m to 3000 m, no change in their characteristics is traceable that would indicate different eruption mechanisms (Fig. 5a). In any case, the deepest cone with a noticeable crater is located in a water depth of ca. 1000 m (marked with a white arrow in Fig. 3c/d).

Deep sea explosive volcanism is usually associated with the exsolution of carbon dioxide (e.g. White et al., 2015). A more detailed explanation was given by Hekinian et al. (2000), who investigated volcanic cones of similar size on the Mid-Atlantic Ridge culminating at depths of 1500 m to 1900 m. There, explosive eruptions were suggested to haven been driven by the superposed effect of magma degassing, first

of the carbon dioxide then of the water content. Since a high volatile content in the Azores magma is described by e.g. Bonatti (1990) and Beier et al. (2012), this mechanism may also be responsible for explosive eruptions in a water depth of >3000 m as postulated in this study. Therefore, deepest explosive structures or deposits in a volcanic setting could generally represent a marker of the volatile content of the corresponding magma source. As an alternative, seawater could be trapped within the cones and vaporized during pulsating magma ascents (Hekinian et al., 2000).

6. Conclusions

252 submarine volcanic cones have been mapped in the submarine domain of the southeastern Terceira Rift. They reveal an average size of (743 ± 405) m in width and (139 ± 77) m in height correlating with slope angles of (20 ± 4)°. They are distributed in water depths of 120 m to 3200 m. Based on a combined morphological and seismic interpretation, all of them are associated with explosive eruptions. Since the cones resemble monogenetic alkali-basaltic cinder cones onshore São Miguel in their topographic appearance, they are assumed to be their submarine equivalent with comparable eruption histories.

Backscatter data shows both a smooth and a rough surface texture, which we expect to be a marker for young or long-time extinguished cones. Currents erode the finer grain-size fraction, so the older the cones are the rougher they become.

The majority of cones can be assigned with one of the following volcanic settings: (1) fault controlled volcanism, where fault planes provide pathways for ascent of magma; (2) parasitic volcanism, where the cones are secondary features of a major subaerial volcanic system; and (3) constructive volcanism, where the cones superimpose a huge submarine volcanic body possibly reflecting a kind of proto-island.

Acknowledgments

We sincerely thank Captain Thomas Wunderlich and his outstanding crew of *RV Meteor* for their support during the M79/2 cruise. We are grateful for the financial support of the German Research Foundation (DFG, grant Hu698/19-1). Additional acknowledgements go to the companies Halliburton-Landmark and Schlumberger for providing university grants for the seismic processing software ProMAX and seismic interpretation software Petrel, respectively, as well as to the NASA's Earth Science Data Systems program for providing the ASTER Global DEM data. Finally, we want to thank P. Nomikou and N.C. Mitchell for reviewing the manuscript. Their suggestions helped a lot to improve this publication.

References

Amante, C., Eakins, B., 2009. ETOPO1 1 arc-minute global relief model: procedures, data sources and analysis. NOAA Technical Memorandum NESDIS NGDC-24 (19 pp.).
Batiza, R., White, J.D., 2000. Submarine lavas and hyaloclastite. Encyclopedia of Volcanoes. Academic Press, San Diego, pp. 361–381.
Beier, C., et al., 2008. Magma genesis by rifting of oceanic lithosphere above anomalous mantle: Terceira Rift, Azores. Geochem. Geophys. Geosyst. 9 (12).
Beier, C., Haase, K.M., Turner, S.P., 2012. Conditions of melting beneath the Azores. Lithos 144–145, 1–11.
Bonatti, E., 1990. Not so hot "hot spots" in the oceanic mantle. Science 250 (4977), 107–111.
Cannat, M., et al., 1999. Mid-Atlantic Ridge–Azores hotspot interactions: along-axis migration of a hotspot-derived event of enhanced magmatism 10 to 4 Ma ago. Earth Planet. Sci. Lett. 173 (3), 257–269.
Casalbore, D., et al., 2015. Volcanic, tectonic and mass-wasting processes offshore Terceira Island (Azores) revealed by high-resolution seafloor mapping. Bull. Volcanol. 77 (3).
Cashman, K.C., Fiske, R.S., 1991. Fallout of pyroclastic debris from submarine volcanic eruptions. Science 253 (5017), 275–280.
Chadwick, W.W., et al., 2008. Direct video and hydrophone observations of submarine explosive eruptions at NW Rota-1 volcano, Mariana arc. J. Geophys. Res. Solid Earth 113 (B8).
Cole, P., Guest, J., Duncan, A., Pacheco, J.-M., 2001. Capelinhos 1957–1958, Faial, Azores: deposits formed by an emergent Surtseyan eruption. Bull. Volcanol. 63 (2–3), 204–220.
Davis, A., Clague, D., 2006. Volcaniclastic deposits from the North Arch volcanic field, Hawaii: explosive fragmentation of alkalic lava at abyssal depths. Bull. Volcanol. 68 (3), 294–307.
Dias, N., et al., 2007. Crustal seismic velocity structure near Faial and Pico Islands (AZORES), from local earthquake tomography. Tectonophysics 445 (3–4), 301–317. http://dx.doi.org/10.1016/j.tecto.2007.09.001.
Eddy, C.A., Dilek, Y., Hurst, S., Moores, E.M., 1998. Seamount formation and associated caldera complex and hydrothermal mineralization in ancient oceanic crust, Troodos ophiolite (Cyprus). Tectonophysics 292 (3–4), 189–210.
Escartín, J., et al., 2001. Crustal thickness of V-shaped ridges south of the Azores: interaction of the Mid-Atlantic Ridge (36°–39°N) and the Azores hot spot. J. Geophys. Res. Solid Earth 106 (B10), 21719–21735.
Fernandes, R., et al., 2006. Defining the plate boundaries in the Azores region. J. Volcanol. Geotherm. Res. 156 (1–2), 1–9. http://dx.doi.org/10.1016/j.jvolgeores.2006.03.019.
Garcia, M.O., et al., 2006. Geology, geochemistry and earthquake history of Loihi Seamount, Hawaii's youngest volcano. Chem. Erde-Geochem. 66 (2), 81–108.
Gente, P., Dyment, J., Maia, M., Goslin, J., 2003. Interaction between the Mid-Atlantic Ridge and the Azores hot spot during the last 85 Myr: emplacement and rifting of the hot spot-derived plateaus. Geochem. Geophys. Geosyst. 4 (10).
Georgen, J.E., Sankar, R.D., 2010. Effects of ridge geometry on mantle dynamics in an oceanic triple junction region: implications for the Azores Plateau. Earth Planet. Sci. Lett. 298 (1–2), 23–34. http://dx.doi.org/10.1016/j.epsl.2010.06.007.
Gregg, T.K.P., Fink, J.H., 1995. Quantification of submarine lava-flow morphology through analog experiments. Geology 23 (1), 73–76.
Griffiths, R.W., Fink, J.H., 1992. Solidification and morphology of submarine lavas: a dependence on extrusion rate. J. Geophys. Res. Solid Earth 97 (B13), 19729–19737.
Hekinian, R., et al., 2000. Deep sea explosive activity on the Mid-Atlantic Ridge near 34°50′N: magma composition, vesicularity and volatile content. J. Volcanol. Geotherm. Res. 98 (1–4), 49–77.
Hübscher, C., 2013. Tragica — Cruise No. M79/2 — August 26–September 21, 2009. Ponta Delgada (Azores / Portugal) — Las Palmas (Canary Islands / Spain). METEOR-Berichte, M79/2, 37 pp., DFG-Senatskommission für Ozeanographie. https://getinfo.de/app/details?id=awi:doi~10.2312%252Fcr_m79_2.
Hübscher, C., Gohl, K., 2014. Reflection/refraction seismology. Encyclopedia of Marine Geosciences. Springer.
Hübscher, C., Ruhnau, M., Nomikou, P., 2015. Volcano-tectonic evolution of the polygenetic Kolumbo submarine volcano/Santorini (Aegean Sea). J. Volcanol. Geotherm. Res. 291, 101–111.
Johnson, C.L., et al., 1998. $^{40}Ar/^{39}Ar$ ages and paleomagnetism of São Miguel lavas, Azores. Earth Planet. Sci. Lett. 160 (3–4), 637–649.
Kokelaar, B., Durant, G.P., 1983. The submarine eruption and erosion of Surtla (Surtsey), Iceland. J. Volcanol. Geotherm. Res. 19 (3–4), 239–246.
Krause, D.C., Watkins, N.D., 1970. North Atlantic crustal genesis in the vicinity of the Azores. Geophys. J. Int. 19 (3), 261–283. http://dx.doi.org/10.1111/j.1365-246X.1970.tb06046.x.
Lourenço, N., et al., 1998. Morpho-tectonic analysis of the Azores Volcanic Plateau from a new bathymetric compilation of the area. Mar. Geophys. Res. Band 20, 141–156.
Luis, J.F., Miranda, J.M., 2008. Reevaluation of magnetic chrons in the North Atlantic between 35°N and 47°N: implications for the formation of the Azores Triple Junction and associated plateau. J. Geophys. Res. Solid Earth Band 113.
Luis, J., Neves, M., 2006. The isostatic compensation of the Azores Plateau: a 3D admittance and coherence analysis. J. Volcanol. Geotherm. Res. Band 156, 10–22.
Luis, J., Miranda, J., Galdeano, A., Patriat, P., 1998. Constraints on the structure of the Azores spreading center from gravity data. Mar. Geophys. Res. 20 (3), 157–170.
Magde, L.S., Smith, D.K., 1995. Seamount volcanism at the Reykjanes Ridge: relationship to the Iceland hot spot. J. Geophys. Res. Solid Earth 100 (B5), 8449–8468.
Marques, F., et al., 2013. GPS and tectonic evidence for a diffuse plate boundary at the Azores Triple Junction. Earth Planet. Sci. Lett. 381, 177–187.
Marques, F., et al., 2014. Corrigendum to "GPS and tectonic evidence for a diffuse plate boundary at the Azores Triple Junction" [Earth Planet. Sci. Lett. 381 (2013) 177–187]. Earth Planet. Sci. Lett. 387 (1), 1–3. http://dx.doi.org/10.1016/j.epsl.2013.11.029.
McKenzie, D., 1972. Active tectonics of the Mediterranean region. Geophys. J. Int. 30 (2), 109–185. http://dx.doi.org/10.1111/j.1365-246X.1972.tb02351.x.
Métrich, N., et al., 2014. Is the 'Azores hotspot' a wetspot? Insights from the geochemistry of fluid and melt inclusions in olivine of Pico basalts. J. Petrol. 55 (2), 377–393. http://dx.doi.org/10.1093/petrology/egt071.
Meyer, J., Mercolli, I., Immenhauser, A., 1996. Off-ridge alkaline magmatism and seamount volcanoes in the Masirah island ophiolite, Oman. Tectonophysics 267 (1–4), 187–208.
Miranda, J., et al., 1998. Tectonic setting of the Azores Plateau deduced from a OBS survey. Mar. Geophys. Res. 20 (3), 171–182.
Miranda, J., Luis, J., Lourenço, N., Goslin, J., 2014. Distributed deformation close to the Azores Triple "Point". Mar. Geol. 355, 27–35.
Mitchell, N.C., et al., 2008. Lava penetrating water: submarine lava flows around the coasts of Pico Island, Azores. Geochem. Geophys. Geosyst. 9 (3).
Mitchell, N.C., et al., 2012. Cone morphologies associated with shallow marine eruptions: east Pico Island, Azores. Bull. Volcanol. 74 (10), 2289–2301.
Mitchell, N.C., Stretch, R., Tempera, F., Ligi, M., 2015. Volcanism in the Azores: a marine geophysical perspective. In: Beier, C., Küppers, U. (Eds.), Volcanism in the Azores. Springer (accepted for publication).
Moore, J.G., 1985. Structure and eruptive mechanisms at Surtsey Volcano, Iceland. Geol. Mag. 11 (Band 122), 649–661.
Moore, R., 1990. Volcanic geology and eruption frequency, São Miguel, Azores. Bull. Volcanol. Band 52, 602–614.

Moore, R.B., Rubin, M., 1991. Radiocarbon dates for lava flows and pyroclastic deposits on São Miguel, Azores. Radiocarbon Band 33 (1), 151–164.
Navarro, A., et al., 2009. Analysis of geometry of volcanoes and faults in Terceira Island (Azores): evidence for reactivation tectonics at the EUR/AFR plate boundary in the Azores triple junction. Tectonophysics 465 (1–4), 98–113.
Németh, K., White, J.D.L., Reay, A., Martin, U., 2003. Compositional variation during monogenetic volcano growth and its implications for magma supply to continental volcanic fields. J. Geol. Soc. Lond. Band 160 (4), 523–530.
Neves, M., Miranda, J., Luis, J., 2013. The role of lithospheric processes on the development of linear volcanic ridges in the Azores. Tectonophysics 608 (0), 376–388.
Nomikou, P., et al., 2012. Submarine volcanoes of the Kolumbo volcanic zone NE of Santorini Caldera, Greece. Glob. Planet. Chang. 90–91, 135–151.
Okubo, C.H., Martel, S.J., 1998. Pit crater formation on Kilauea volcano, Hawaii. J. Volcanol. Geotherm. Res. 86 (1–4), 1–18.
Robertson, A.H., 1998. Mesozoic–Tertiary tectonic evolution of the easternmost Mediterranean area: integration of marine and land evidence. Proc. Ocean Drill. Program Sci. Results Band 160 (Chapter 54).
Rubin, K.H., et al., 2012. Volcanic eruptions in the deep sea. Oceanogr. Band 25 (1), 142–157.
Sansone, F.J., Smith, J.R., 2006. Rapid mass wasting following nearshore submarine volcanism on Kilauea volcano, Hawaii. J. Volcanol. Geotherm. Res. 151 (1–3), 133–139.
Schilling, J.-G., 1975. Azores mantle blob: rare-earth evidence. Earth Planet. Sci. Lett. 25 (2), 103–115.
Schmincke, H.-U., 2005. Volcanism. Springer.
Searle, R., 1980. Tectonic pattern of the Azores spreading centre and triple junction. Earth Planet. Sci. Lett. 51 (2), 415–434. http://dx.doi.org/10.1016/0012-821X(80)90221-6.
Sibrant, A., et al., 2015. Morpho-structural evolution of a volcanic island developed inside an active oceanic rift: S. Miguel Island (Terceira Rift, Azores). J. Volcanol. Geotherm. Res. 301, 90–106.
Silveira, G., et al., 2010. Stratification of the Earth beneath the Azores from P and S receiver functions. Earth Planet. Sci. Lett. 299 (1–2), 91–103. http://dx.doi.org/10.1016/j.epsl.2010.08.021.
Smith, D.K., 1996. Comparison of the shapes and sizes of seafloor volcanoes on Earth and "pancake" domes on Venus. J. Volcanol. Geotherm. Res. 73 (1–2), 47–64.
Smith, T., Batiza, R., 1989. New field and laboratory evidence for the origin of hyaloclastite flows on seamount summits. Bull. Volcanol. 51 (2), 96–114.
Smith, D.K., Cann, J.R., 1999. Constructing the upper crust of the Mid-Atlantic Ridge: a reinterpretation based on the Puna Ridge, Kilauea Volcano. J. Geophys. Res. Solid Earth 104 (B11), 25379–25399.
Smith, D.K., et al., 1995a. Mid-Atlantic Ridge volcanism from deep-towed side-scan sonar images, 25°–29°N. J. Volcanol. Geotherm. Res. 67 (4), 233–262.
Smith, D.K., Humphris, S.E., Bryan, W.B., 1995b. A comparison of volcanic edifices at the Reykjanes Ridge and the Mid-Atlantic Ridge at 24°–30°N. J. Geophys. Res. Solid Earth 100 (B11), 22485–22498.
Sohn, R.A., et al., 2008. Explosive volcanism on the ultraslow-spreading Gakkel ridge, Arctic Ocean. Nature Band 453, 1236–1238.
Solgevik, H., Mattsson, H.B., Hermelin, O., 2007. Growth of an emergent tuff cone: fragmentation and depositional processes recorded in the Capelas tuff cone, São Miguel, Azores. J. Volcanol. Geotherm. Res. 159 (1–3), 246–266.
Stretch, R., Mitchell, N., Portaro, R., 2006. A morphometric analysis of the submarine volcanic ridge south-east of Pico Island, Azores. J. Volcanol. Geotherm. Res. 156 (1–2), 35–54.
Tempera, F., et al., 2013. Condor seamount (Azores, NE Atlantic): a morpho-tectonic interpretation. Deep-Sea Res. II Top. Stud. Oceanogr. 98 (0), 7–23 (Part A).
Weiß, B., Hübscher, C., Lüdmann, T., 2015. The tectonic evolution of the southeastern Terceira Rift/São Miguel region (Azores). Tectonophysics 654, 75–95.
White, J.D., Schipper, C.I., Kano, K., 2015. Submarine explosive eruptions (Chapter 31) In: Sigurdsson, H. (Ed.), The Encyclopedia of Volcanoes, 2nd ed. Academic Press Amsterdam, pp. 553–569.
Wood, C.A., 1980. Morphometric evolution of cinder cones. J. Volcanol. Geotherm. Res. 7 (3–4), 387–413.
Yang, T., et al., 2006. Upper mantle structure beneath the Azores hotspot from finite-frequency seismic tomography. Earth Planet. Sci. Lett. 250 (1–2), 11–26.